

Nanosecond Folding Dynamics of a Three-Stranded β -Sheet

Yao Xu, Pradipta Purkayastha, and Feng Gai*

Contribution from the Department of Chemistry, University of Pennsylvania, Philadelphia, Pennsylvania 19104

Received July 8, 2006; E-mail: gai@sas.upenn.edu

Abstract: We studied conformational stability and folding kinetics of a three-stranded β -sheet containing two rigid turns. Static infrared measurements indicate that this β -sheet undergoes a broad but cooperative thermal unfolding transition with a midpoint at ~ 53 °C. Interestingly, time-resolved infrared experiments show that its relaxation kinetics in response to a temperature-jump (T -jump) occur on the nanosecond time scale (e.g., the relaxation time is ~ 140 ns at 35.0 °C), thereby suggesting that the conformational relaxation encounters only a small free energy barrier or even proceeds in a downhill manner. Further Langevin dynamics simulations suggest that the observed T -jump relaxation kinetics could be modeled by a conformational diffusion process along a single-well free energy profile, which allowed us to determine the effective diffusion constant and also the roughness of the folding energy landscape.

Introduction

Recently, there has been an increased interest in identifying and designing single-domain proteins that fold on the ultrafast time scale.^{1–8} The goal is not only to provide model systems for computer simulations but also to understand determinants of protein folding kinetics, such as the folding “speed limit”.^{1–5} The latter may be interpreted as the fundamental rate in protein folding dynamics because it is analogous to the pre-exponential factor of transition state theory rate constant, i.e., $k_B T/h$. Until now, a number of proteins composed of predominantly helical secondary structures have been shown to fold in less than ten microseconds,^{2–5,7} providing an estimate of the folding speed limit for helical proteins. The reason that those proteins can fold extremely fast may well be related to the fact that folding of individual helices occurs on a time scale of about 100–500 ns, depending on temperature, sequence, and chain length.^{9–12}

However, most β -hairpins fold at least 10 times slower than monomeric helices, suggesting that the native state topology is an important determinant of the folding energy landscape.¹³

Recently, Du et al. have shown that the entropic cost associated with the turn formation could dominate the total free energy barrier in β -hairpin folding.¹⁴ Their results indicated that the folding rate of a β -hairpin could be fine-tuned by varying its turn sequence. Given the fact that the energetic barrier for β -hairpin folding is small,^{15–17} this may prove to be an effective means to design or identify β -sheet sequences that are capable of ultrafast folding. For example, the folding process of β -sheet proteins containing rigid turns that are predisposed to fold in the unfolded states could encounter only a small free energy barrier or even proceed in a downhill manner.

Downhill or “type 0” protein folding process has been predicted by the energy landscape theory^{18,19} and studied through experiments.^{2,20–22} A downhill folding process does not involve crossing over distinct free energy barriers, thereby exhibiting unique behaviors that are different from those associated with a two-state folding mechanism where a single free energy barrier separates the folded from the unfolded states. A downhill folder could be used to study some fundamental properties of the folding free energy landscape that are not attainable from scrutinizing two-state folding kinetics.^{2,21,22} For example, it may allow one to determine not only the fundamental rate in protein folding but also the roughness of the folding free energy landscape.²¹

- (1) Eaton, W. A. *Proc. Natl. Acad. Sci. U.S.A.* **1999**, *96*, 5897–5899.
- (2) Yang, W. Y.; Gruebele, M. *Nature* **2003**, *423*, 193–197.
- (3) Zhu, Y.; Alonso, D. O. V.; Maki, K.; Huang, C.-Y.; Lahr, S. J.; Daggett, V.; Roder, H.; DeGrado, W. F.; Gai, F. *Proc. Natl. Acad. Sci. U.S.A.* **2003**, *100*, 15486–15491.
- (4) Kubelka, J.; Hofrichter, J.; Eaton, W. A. *Curr. Opin. Struct. Biol.* **2004**, *14*, 76–88.
- (5) Zhu, Y.; Fu, X.; Wang, T.; Tamura, A.; Takada, S.; Saven, J. G.; Gai, F. *Chem. Phys.* **2004**, *307*, 99–109.
- (6) Faraone-Mennella, J.; Gray, H. B.; Winkler, J. R. *Proc. Natl. Acad. Sci. U.S.A.* **2005**, *102*, 6315–6319.
- (7) Chiu, T. K.; Kubelka, J.; Herbst-Irmer, R.; Eaton, W. A.; Hofrichter, J.; Davies, D. R. *Proc. Natl. Acad. Sci. U.S.A.* **2005**, *102*, 7517–7522.
- (8) Bunagan, M. R.; Yang, X.; Saven, J. G.; Gai, F. *J. Phys. Chem. B* **2006**, *110*, 3759–3763.
- (9) Williams, S.; Causgrove, T. P.; Gilmanshin, R.; Fang, K. S.; Callender, R. H.; Woodruff, W. H.; Dyer, R. B. *Biochemistry* **1996**, *35*, 691–697.
- (10) Eaton, W. A.; Muñoz, V.; Thompson, P. A.; Henry, E. R.; Hofrichter, J. *Acc. Chem. Res.* **1998**, *31*, 745–753.
- (11) Huang, C.-Y.; Klemke, J. W.; Getahun, Z.; DeGrado, W. F.; Gai, F. *J. Am. Chem. Soc.* **2001**, *123*, 9235–9238.
- (12) Wang, T.; Zhu, Y.; Getahun, Z.; Du, D.; Huang, C.-Y.; DeGrado, W. F.; Gai, F. *J. Phys. Chem. B* **2004**, *108*, 15301–15310.

- (13) Plaxco, K. W.; Simons, K. T.; Baker, D. *J. Mol. Biol.* **1998**, *277*, 985–994.
- (14) Du, D.; Tucker, M. J.; Gai, F. *Biochemistry* **2006**, *45*, 2668–2678.
- (15) Muñoz, V.; Thompson, P. A.; Hofrichter, J.; Eaton, W. A. *Nature* **1997**, *390*, 196–199.
- (16) Xu, Y.; Oyola, R.; Gai, F. *J. Am. Chem. Soc.* **2003**, *125*, 15388–15394.
- (17) Du, D.; Zhu, Y.; Huang, C.-Y.; Gai, F. *Proc. Natl. Acad. Sci. U.S.A.* **2004**, *101*, 15915–15920.
- (18) Bryngelson, J. D.; Onuchic, J. N.; Succi, N. D.; Wolynes, P. G. *Proteins Struct. Funct. Genet.* **1995**, *21*, 167–195.
- (19) Onuchic, J. N.; Wolynes, P. G. *Curr. Opin. Struct. Biol.* **2004**, *14*, 70–75.
- (20) Garcia-Mira, M. M.; Sadqi, M.; Fischer, N.; Sanchez-Ruiz, J. M.; Muñoz, V. *Science* **2002**, *298*, 2191–2195.
- (21) Yang, W. Y.; Gruebele, M. *Biophys. J.* **2004**, *87*, 596–608.
- (22) Ma, H.; Gruebele, M. *Proc. Natl. Acad. Sci. U.S.A.* **2005**, *102*, 2283–2287.

Table 1. The Sequence of $^{\text{D}}\text{P}^{\text{D}}\text{P}$ -II and Its Mutants

peptide	sequence ^a
$^{\text{D}}\text{P}^{\text{D}}\text{P}$ -II	R-Phe-IEV ^D PGKKFITS ^D PGKT-Tyr-TE
$^{\text{D}}\text{P}^{\text{D}}\text{P}$ -II-m1	R-Phe [*] -IEV ^D PGKKFITS ^D PGKT-Trp-TE
$^{\text{D}}\text{P}^{\text{D}}\text{P}$ -II-m2	R-Phe [*] -IEV ^D PGKKFITS ^D PGKT-Phe-TE

^a Phe* represents Phe_{CN}

D-Proline ($^{\text{D}}\text{P}$) is commonly used to enhance the conformational stability of designed β -sheets.²³ This is because the molecular geometry of $^{\text{D}}\text{P}$ is compatible with the right-handed twist of the β -sheet structure,²⁴ and thus, it can effectively reduce the entropic cost associated with the turn formation²³ and consequently increase the stability of the folded state by increasing the folding rate.¹⁷ Therefore, antiparallel β -sheets containing a $^{\text{D}}\text{P}$ residue in their turn sequence are potential candidates for exhibiting ultrafast or even downhill folding behaviors. For example, Du et al.¹⁷ have shown that, among four 12-residue β -hairpins differing only in their turn sequences, the one containing a $^{\text{D}}\text{P}$ turn segment exhibits the fastest folding rate. Similarly, Nguyen et al.²⁵ have shown that the folding rate of the hPin1 WW domain could be sped up by an order of magnitude simply by mutating four native residues in its loop I to $^{\text{D}}\text{P}$. Herein, we investigated thermodynamics and kinetics of a $^{\text{D}}\text{P}$ -containing peptide originally designed by Gellman and co-workers,²⁶ who have shown that this peptide (i.e., $^{\text{D}}\text{P}^{\text{D}}\text{P}$ -II in Table 1) folds into a three-stranded antiparallel β -sheet conformation in aqueous solution. Due to the high turn-forming propensity of the $^{\text{D}}\text{P}$ turn segments in $^{\text{D}}\text{P}^{\text{D}}\text{P}$ -II, this β -sheet is fairly stable. Consistent with our speculation, time-resolved infrared (IR) measurements indicate that the relaxation kinetics of $^{\text{D}}\text{P}^{\text{D}}\text{P}$ -II in response to a T -jump are extremely fast, on the nanosecond time scale, thereby suggesting that its folding encounters either a relatively small free energy barrier between two distinguishable conformational states or no distinct barriers at all, i.e., a downhill folding without traditionally defined folded and unfolded states. To understand these results, we have analyzed the T -jump induced relaxation kinetics according to two different scenarios. A two-state analysis allowed us to explicitly determine the temperature-dependent folding rate, whereas Langevin dynamics simulations where folding was assumed to proceed along a one-dimensional, barrierless free energy surface allowed us to determine the roughness of the folding potential. Although we were unable to distinguish between these two possibilities, this study nevertheless revealed information that is important for understanding the folding dynamics of β -sheet conformations.

It appears that we can attribute the ultrafast relaxation behavior of $^{\text{D}}\text{P}^{\text{D}}\text{P}$ -II to its $^{\text{D}}\text{P}$ turn segment, which has been shown to be able to form a type II' turn that is extremely tolerant to various denaturation conditions.^{27,28} Hence, we expect that the turn conformations of $^{\text{D}}\text{P}^{\text{D}}\text{P}$ -II do not show significant changes within the temperature range in which the T -jump data

were collected. Consequently, the compactness of this peptide should exhibit modest temperature dependence. To verify this hypothesis, we further employed a fluorescence resonance energy transfer (FRET) method to evaluate how the compactness of $^{\text{D}}\text{P}^{\text{D}}\text{P}$ -II changes as a function of temperature. Our results indeed show that the distance between the donor and acceptor, which are located at the N- and C-terminus strands, respectively, does not change significantly with increasing temperature.

Materials and Methods

Samples. Peptides were synthesized using the standard fluoren-9-ylmethoxycarbonyl based solid-phase method on Rink resin, purified by reverse-phase chromatography. The identity of each peptide was further verified by matrix-assisted laser desorption ionization mass spectroscopy. The residual trifluoroacetic acid from peptide synthesis, which has an IR band at 1672 cm^{-1} , was removed by multiple lyophilizations against a 0.1 M DCl solution. For both equilibrium and time-resolved IR experiments, the sample was prepared by directly dissolving the lyophilized peptide solid in D_2O and the final concentration was 2–3 mM.

Infrared Measurements. FTIR spectra were collected on a Nicolet Magna-IR 860 spectrometer using 1 cm^{-1} spectral resolution. A thermostated and two-compartment CaF_2 sample cell with a 52 μm optical path length was used to measure the temperature-dependent FTIR spectra of the sample and reference (D_2O) under identical conditions. The laser-induced T -jump infrared setup has been described in detail elsewhere.¹¹ Briefly, a 3 ns, 1.92 μm pulse was used to generate a T -jump and the resultant transient absorbance change was detected by a CW lead salt infrared diode laser in conjunction with a 50 MHz MCT detector.

FRET Measurements. Fluorescence spectra were obtained on a Fluorolog 3.10 spectrofluorometer (Jobin Yvon Horiba, NJ) with 1 nm spectral resolution (excitation and emission) and a 1 cm quartz sample cuvette. Temperature was regulated using a TLC 50 Peltier temperature controller (Quantum Northwest, WA). The peptide sample was prepared by directly dissolving lyophilized solids into H_2O and the final concentration was around 20 μM , determined optically using $\epsilon_{280} = 850 \text{ M}^{-1} \text{ cm}^{-1}$ for the reference peptide ($^{\text{D}}\text{P}^{\text{D}}\text{P}$ -II-m2) and $\epsilon_{280} = 5690 \text{ M}^{-1} \text{ cm}^{-1}$ for $^{\text{D}}\text{P}^{\text{D}}\text{P}$ -II-m1. Temperature-dependent fluorescence spectra in the spectral range of 250–450 nm were collected from 0 to 95 $^{\circ}\text{C}$, in a step of 5 $^{\circ}\text{C}$, with an excitation wavelength of 240 nm. The FRET efficiency, E , was calculated according to the following equation:

$$E = \frac{I_{\text{D}} - I_{\text{DA}}}{I_{\text{D}}} \quad (1)$$

where I_{DA} and I_{D} are the integrated fluorescence intensities of the donor, with and without the presence of the acceptor, respectively. For the current study, I_{DA} corresponds to the integrated area of the Phe_{CN} fluorescence spectrum obtained with $^{\text{D}}\text{P}^{\text{D}}\text{P}$ -II-m1 peptide, and I_{D} corresponds to that obtained with the reference peptide $^{\text{D}}\text{P}^{\text{D}}\text{P}$ -II-m2, under the same conditions. To accurately determine the integrated area of the Phe_{CN} fluorescence,²⁹ which overlaps the emission spectrum of Trp, we fit the fluorescence spectrum of these peptides by using a linear combination of two profiles generated from fitting the fluorescence spectra of Trp and Phe_{CN} plus a linear background.

Langevin Dynamics Simulations. The T -jump induced conformational kinetics of $^{\text{D}}\text{P}^{\text{D}}\text{P}$ -II at selected final temperatures were modeled by Langevin dynamics in the high friction limit. For simplicity, the conformational motion was assumed to occur on a one-dimensional free energy surface, $G(q)$,

(23) Espinosa, J. F.; Syud, F. A.; Gellman, S. H. *Protein Sci.* **2002**, *11*, 1492–1505.

(24) Chothia, C. *J. Mol. Biol.* **1973**, *75*, 295–302.

(25) Nguyen, H.; Jäger, M.; Kelly, J. W.; Grubele, M. *J. Phys. Chem. B* **2005**, *109*, 15182–15186.

(26) Syud, F. A.; Stanger, H. E.; Schenck, Mortell, H.; Espinosa, J. F.; Fisk, J. D.; Fry, C. G.; Gellman, S. H. *J. Mol. Biol.* **2003**, *326*, 553–568.

(27) Kuznetsov, S. V.; Hilario, J.; Keiderling, T. A.; Ansari, A. *Biochemistry* **2003**, *42*, 4321–4332.

(28) Hilario, J.; Kubelka, J.; Keiderling, T. A. *J. Am. Chem. Soc.* **2003**, *125*, 7562–7574.

(29) Tucker, M. J.; Oyola, R.; Gai, F. *J. Phys. Chem. B* **2005**, *109*, 4788–4795.

$$G(q) = 10(q-1)^2 \times H(q-1) + 0.5(q-1)^2 \times H(q-0.5) \times H(1-q) + (1-q^2)/6 \times H(0.5-q) \times H(q+0.5) + 0.5(q+1)^2 \times H(-q-0.5) \times H(-q-1) + 0.5(q+1)^2 \times H(-q-1) + A(T) \times (q-1) + \Delta G_{\text{ran}} \quad (2)$$

where q is the reaction coordinate and is related to the IR observable used in the current study. $H(q)$ is the Heaviside function, and ΔG_{ran} represents the intrinsic roughness of the free energy surface. $A(T)$ is a function of temperature and is adjusted to match the equilibrium populations obtained from the equilibrium FTIR experiments. The latter was achieved by assuming that conformations with $q > 0.7$ would give rise to the characteristic amide I' band of antiparallel β -sheet. We found that $A(T)$ is a nonlinear function of T over a broad temperature range. However, between 20 and 60 °C $A(T)$ depends approximately linearly on temperature (see below). The dynamics of the T -jump induced population redistribution on a new free energy surface, which is determined by the final temperature, were evaluated using the following equation,

$$\frac{k_B T}{D} \frac{\partial q}{\partial t} = - \frac{\partial G(q)}{\partial q} + \Gamma(t) \quad (3)$$

where D is the diffusion constant and $\Gamma(t)$ represents the fluctuating force exerted by the thermal bath. This diffusion equation was numerically solved using a fourth-order Runge–Kutta algorithm in Matlab (Mathworks, Natick, MA). In one type of simulation, ΔG_{ran} was set as zero. Whereas in another type of simulation, ΔG_{ran} was mimicked by Gaussian random noise with a root-mean-square of $\epsilon^2 k_B^2 T^2$, which was assumed to be independent of the reaction coordinate. ΔG_{ran} is rescaled to reproduce the kinetic data for a given D , which was set as $0.04 \text{ nm}^2/\text{ns}^{30,31}$ in the current study and the free energy fluctuation δG is expressed as $\epsilon k_B T$. To compare the calculated population relaxations with experimental relaxation kinetics, the time-dependent population distribution function $p(q,t)$ is further converted to a kinetic signal $S(t)$ using the following equation:

$$S(t) = \int H(q-0.7)p(q,t) dq \quad (4)$$

where the Heaviside function $H(q-0.7)$ ($= 0$ if $q \leq 0.7$; $= 1$ if $q > 0.7$), which is used as a step switching function for calculating the IR kinetics, is the same as that used in the equilibrium calculation.

Results

The 20-residue $\text{D}^{\text{p}}\text{D}^{\text{p}}\text{-II}$ peptide was synthesized based on the sequence designed by Gellman and co-workers.²⁶ We made a minor modification to the original peptide sequence wherein the unnatural amino acid ornithine, which was used to maximize the NMR signals,^{26,32} was mutated to lysine because it has been shown that both amino acids show similar β -sheet propensities.^{26,32}

The thermal unfolding transition of $\text{D}^{\text{p}}\text{D}^{\text{p}}\text{-II}$ was studied using FTIR spectroscopy. As shown (Figure 1), its amide I' band, which mainly arises from the stretching vibration of backbone C=O's, consists of four overlapping but resolvable spectral components. The spectral features centered at ~ 1634 and $\sim 1678 \text{ cm}^{-1}$ are due to various coupling mechanisms among individual amide carbonyls^{33,34} and have been shown to

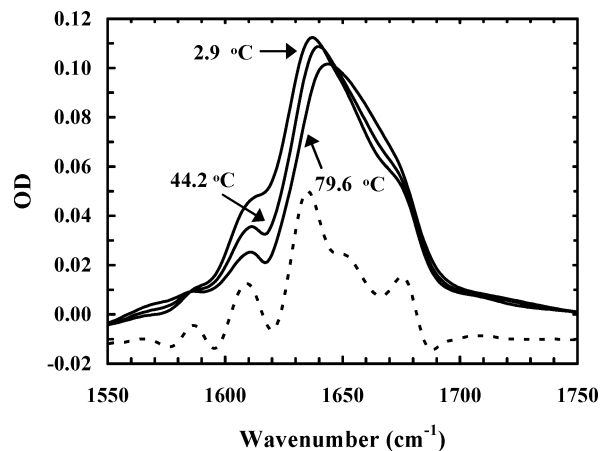


Figure 1. Representative FTIR spectra (solid lines) of $\text{D}^{\text{p}}\text{D}^{\text{p}}\text{-II}$ in D_2O ($\text{pH}^* 4.5$) at 2.9, 44.2, 79.6 °C, as indicated. Also shown (dashed line) is the resolution-enhanced FTIR spectrum at 2.9 °C, which was achieved by Fourier self-deconvolution using an enhancement factor of 2 and a bandwidth of 18 cm^{-1} .

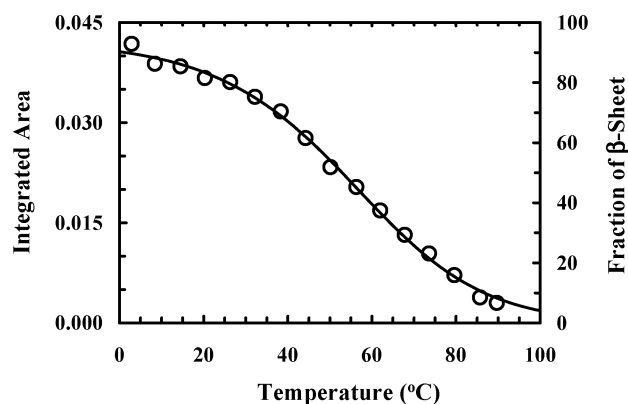


Figure 2. Integrated area of the 1678 cm^{-1} band (left y-axis) and the fraction of β -sheet (right y-axis) vs temperature (open cycle). Fitting these data to a two-state model (solid line) with temperature-independent folded and unfolded baselines yields the following thermodynamic parameters for unfolding: $\Delta H_m = 12.3 \pm 0.9 \text{ kcal mol}^{-1}$, $\Delta S_m = 37.7 \pm 2.8 \text{ cal mol}^{-1} \text{ K}^{-1}$, $\Delta C_p = 173 \pm 15 \text{ cal mol}^{-1} \text{ K}^{-1}$ and $T_m = 52.6 \pm 0.4 \text{ °C}$.

be characteristic IR markers of antiparallel β -sheets.³⁵ Consistently, the difference spectra computed from these FTIR spectra (data not shown) indicate that the intensities of these bands decrease with increasing temperature, owing to the decreased β -sheet content at higher temperatures. Keiderling and co-workers have shown that the band centered at $\sim 1610 \text{ cm}^{-1}$ can be assigned to the amide C=O of the D^{p} residue.^{27,28} Indeed, the band area of this component, obtained from curve fitting, accounts for about 13% of the total amide I' band area of $\text{D}^{\text{p}}\text{D}^{\text{p}}\text{-II}$, in good agreement with the percentage of the D^{p} residue in $\text{D}^{\text{p}}\text{D}^{\text{p}}\text{-II}$ sequence.

To quantify the thermal unfolding transition of $\text{D}^{\text{p}}\text{D}^{\text{p}}\text{-II}$, we have employed a global fitting method^{16,17} to determine the temperature dependent integrated area of the 1678 cm^{-1} band from the corresponding FTIR difference spectra. As shown (Figure 2), the integrated area of this band, which is proportional to the antiparallel β -sheet content, decreases with increasing temperature. Although the thermal unfolding transition revealed by this band is broad, it can be described by an apparent two-state model. On the basis of the method proposed by Klimov

(30) Buckler, D. R.; Hass, E.; Scheraga, H. A. *Biochemistry* **1995**, *34*, 15965–15978.

(31) Hagen, S. J.; Hofrichter, J.; Eaton, W. A. *J. Phys. Chem. B* **1997**, *101*, 2352–2356.

(32) Syud, F. A.; Espinosa, J. F.; Gellman, S. H. *J. Am. Chem. Soc.* **1999**, *121*, 11577–11578.

(33) Miyazawa, T.; Blout, E. R. *J. Am. Chem. Soc.* **1961**, *83*, 712–719.

(34) Moore, W. H.; Krimm, S. *Proc. Natl. Acad. Sci. U.S.A.* **1975**, *97*, 4933–4935.

(35) Surewicz, W. K.; Mantsch, H. H.; Chapman, D. *Biochemistry* **1993**, *32*, 389–394.

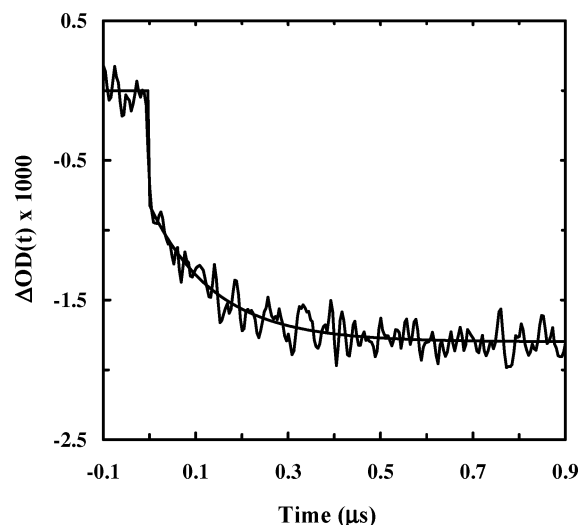


Figure 3. Representative relaxation kinetic trace probed at 1633 cm^{-1} for $\text{D}^{\text{PDP}}\text{-II}$ in response to a T -jump of 25.4 to $35.0\text{ }^{\circ}\text{C}$. The smooth line is the fit to the following function, $\text{OD}(t) = A[1 - B \cdot \exp(-t/\tau)]$, with $A = -1.8$, $B = 0.54$, and $\tau = 0.14 \pm 0.02\ \mu\text{s}$, convolved with the instrument response function determined from the risetime of the buffer temperature.

and Thirumalai,³⁶ the width of the transition (i.e., the full width at half-maximum of the $d[\beta]/dT$ profile) was determined to be $\sim 59\text{ }^{\circ}\text{C}$, indicative of a weak but cooperative transition.

The T -jump induced relaxation kinetics of $\text{D}^{\text{PDP}}\text{-II}$ were studied by an IR method.¹¹ Similar to those observed for other β -sheet systems,^{14,16,17,37} the T -jump IR kinetics of $\text{D}^{\text{PDP}}\text{-II}$ contain two distinctive phases (Figure 3). According to our early interpretation,³⁷ the fast phase, which was too fast to be resolved by the current setup, was assigned to spectral changes that are not associated with the global folding/unfolding of the peptide. Because the amide I band of proteins and peptides depends on the hydration status of the “exposed” amide groups, changing temperature affects its absorption profile.³⁸ Therefore, a T -jump would produce an unresolved IR kinetic phase because such temperature-induced spectral changes occur on a time scale that is faster than the time resolution of the current setup.^{37,39,40} The slow phase was resolvable for final temperatures below $55\text{ }^{\circ}\text{C}$ and could be adequately modeled by a single-exponential function. Because a two-state folder always yields a single-exponential relaxation in response to a perturbation, this result is thereby consistent with (but not necessarily indicative of) a two-state folding scenario wherein a single free energy barrier distinctly separates the folded $\text{D}^{\text{PDP}}\text{-II}$ from its thermally unfolded counterpart. Furthermore, the ultrafast (i.e., nano-second) relaxation behavior of $\text{D}^{\text{PDP}}\text{-II}$ in response to a T -jump (Figure 3) suggests that the corresponding conformational process encounters only a relatively small, if any, free energy barrier.

To facilitate understanding of ultrafast relaxation behavior of $\text{D}^{\text{PDP}}\text{-II}$, we further investigated the effect of temperature on its compactness using a FRET technique whereby an amino

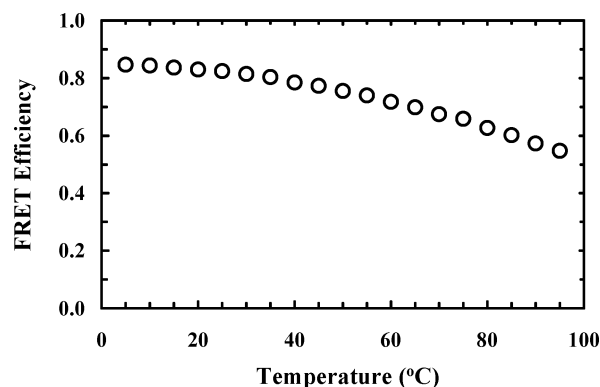


Figure 4. FRET efficiency of $\text{D}^{\text{PDP}}\text{-II-m1}$ vs temperature.

acid FRET pair, p -cyano-phenylalanine (Phe_{CN}) and tryptophan (Trp), was used. Tucker et al.²⁹ have recently shown that Phe_{CN} can be used as a FRET donor to Trp and have applied this FRET pair to study the conformational distribution of a 14-residue unstructured peptide²⁹ and also the thermal unfolding transition of a 16-residue β -hairpin.¹⁴ To utilize this FRET pair, we synthesized a double mutant of $\text{D}^{\text{PDP}}\text{-II}$, i.e., $\text{F2Phe}_{\text{CN}}/\text{Y18W}$ (i.e., $\text{D}^{\text{PDP}}\text{-II-m1}$ in Table 1). FTIR studies indicate that $\text{D}^{\text{PDP}}\text{-II-m1}$ adopts an antiparallel β -sheet conformation and exhibits a thermal unfolding transition very similar to that of the wild type (data not shown). As shown (Figure 4), the FRET efficiency of $\text{D}^{\text{PDP}}\text{-II-m1}$, calculated based on the method described in the Materials and Methods section and the fluorescence of a reference peptide, $\text{D}^{\text{PDP}}\text{-II-m2}$, only changes modestly from 0 to $95\text{ }^{\circ}\text{C}$. This result indicates that the separation distance between the donor and acceptor, which could be used as a measure of the compactness of $\text{D}^{\text{PDP}}\text{-II-m1}$, does not vary significantly in this temperature range. Consistent with this observation, the results of Kuznetsov et al.²⁷ also suggest that peptide D^{PDP} , which has the same turn sequence to that of $\text{D}^{\text{PDP}}\text{-II}$, remains highly compact even under high denaturation conditions.²⁷ Therefore, the relative compact conformation adopted by $\text{D}^{\text{PDP}}\text{-II-m1}$, even at temperatures where the β -sheet content is small, appears to arise from the intrinsic rigidity of the stable β -turn formed by the D^{PG} segment, which could constrain the flexibility of the polypeptide chain. Because of the similarity in the sequences of $\text{D}^{\text{PDP}}\text{-II-m1}$ and $\text{D}^{\text{PDP}}\text{-II}$, it is reasonable to assume that the latter also adopts a compact structure even under thermal denaturation conditions.

Discussion

Although the folded state of $\text{D}^{\text{PDP}}\text{-II}$ consists of three β -strands, its conformational relaxation in response to a T -jump is much faster than that of β -hairpins.^{14–17} For instance, the relaxation rate of $\text{D}^{\text{PDP}}\text{-II}$ is $(0.14 \pm 0.02\ \mu\text{s})^{-1}$ at $35.0\text{ }^{\circ}\text{C}$, which is not only the fastest T -jump relaxation rate observed for a β -sheet system so far, but is also comparable to that observed for monomeric α -helices,^{9–12} the folding of which mostly involves local interactions. These results suggest that the T -jump induced relaxation in $\text{D}^{\text{PDP}}\text{-II}$ does not involve large-amplitude conformational motions, and as a result, the structural evolution can proceed quickly to the new equilibrium position. In other words, our results suggest that the radius of gyration or compactness of the conformational ensembles involved in such relaxations, namely those corresponding to the initial and final temperatures, is similar. Consistent with this

(36) Klimov, D. K.; Thirumalai, D. *Proc. Natl. Acad. Sci. U.S.A.* **2000**, *97*, 2544–2549.

(37) Xu, Y.; Wang, T.; Gai, F. *Chem. Phys.* **2006**, *323*, 21–27.

(38) Walsh, S. T. R.; Cheng, R. P.; Wright, W. W.; Alonso, D. O. V.; Daggett, V.; Vanderkooi, J. M.; DeGrado, W. F. *Protein Sci.* **2003**, *12*, 520–531.

(39) Volk, M.; Kholodenko, Y.; Lu, H. S. M.; Gooding, E. A.; DeGrado, W. F.; Hochstrasser, R. M. *J. Phys. Chem. B* **1997**, *101*, 8607–8616.

(40) Bredenbeck, J.; Helbing, J.; Kumita, J. R.; Woolley, G. A.; Hamm, P. *Proc. Natl. Acad. Sci. U.S.A.* **2005**, *102*, 2379–2384.

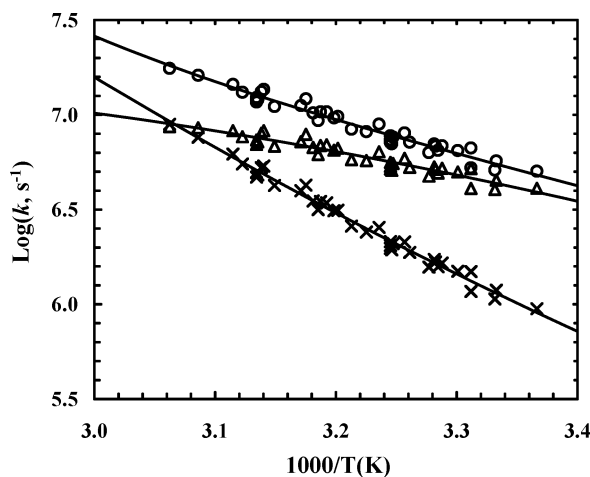


Figure 5. Arrhenius plot of the measured relaxation rate constants (O) and also the folding (Δ) and unfolding (x) rate constants obtained from a two-state analysis. Lines are fits to the Eyring equation.

picture, our FRET results indicate that the separation distance between the Phe_{CN} and Trp, which are located near the N- and C-termini of ^DPDP-II-m1, respectively, only changes modestly within the temperature range of 0–95 °C (Figure 4). Qualitatively speaking, these FRET data are supportive of the idea that the *T*-jump induced structural evolution in ^DPDP-II involves a (relatively) short path because the conformational search is limited in a compact space, similar to the notion that an initial collapse process could effectively reduce the conformational space that a protein has to search and, thereby, speeding up folding.⁴¹ Although several types of interactions can lead to the formation of a collapsed or compact conformation, we believe that in the current case it is the ^DPG turn that causes ^DPDP-II-m1 and also ^DPDP-II to adopt a compact structure, even under highly denatured conditions. Comparative studies have shown that ^DPG has a very high turn propensity when placed at the center of a loop sequence,^{23,28} partly due to the fact that the molecular geometry of the ^DP residue is compatible with the right-handed twist of the β -sheet^{24,42} and is ideal for the *i*+1 position of a type I' or type II' β -turn. Therefore, a turn formed by a sequence containing ^DPG cannot be easily disrupted and could be maintained even at conditions where other secondary structures are lost.⁴² For this reason, ^DPG is often used in designed β -sheets^{23,26,42} because its intrinsic rigidity helps reduce the entropic cost associated with the turn formation²³ and consequently stabilizes the folded state by increasing the folding rate.¹⁷

If we were to assume that the folding-unfolding transition of ^DPDP-II follows a two-state mechanism, the measured relaxation rate constant (k_R) could be further separated into the corresponding folding (k_f) and unfolding (k_u) rate constants using the thermodynamic parameters determined from FTIR measurements (Figure 2) in conjunction with the following relationships: $k_R = k_f + k_u$ and $K_{eq} = k_u/k_f$, where K_{eq} is the equilibrium constant for unfolding. As shown (Figure 5), such an analysis yielded a folding rate constant that is only weakly temperature dependent, similar to that observed for other β -sheets.^{14,16,17} However, the folding rate extracted from such a two-state analysis is extremely fast, e.g., $(0.26 \pm 0.02 \mu\text{s})^{-1}$ at 25 °C.

Considering the fact that this rate is comparable to that of the helix-coil transition^{9–12} but is much faster than that of β -hairpin formation,^{14–17} this result suggests that the folding free energy barrier encountered by the ‘thermally unfolded states’ of ^DPDP-II must be relatively small. This result is in agreement with several previous studies that demonstrated that turn formation nucleates the folding^{43,44} of β -sheets and is the rate-limiting step.^{14,17,45} As suggested by the above FRET results and also a NMR study,²³ the ^DPG segment helps form a rigid and stable turn that may resist thermal denaturation. Hence, the entropic penalty associated with the search for the native turn conformations in the folding process of ^DPDP-II from its “thermally unfolded states” is expected to be greatly reduced. Also consistent with this notion, a recent study regarding the effect of the Pro residue on the loop formation rate indicated that short loops are formed fastest around *cis*-prolyl bonds due to the largely restricted conformational space.⁴⁶ Finally, globally fitting these two-state folding and unfolding rate constants to the Eyring equation¹⁷ yielded an apparent enthalpy of activation (ΔH^\ddagger) of 4.4 ± 0.4 kcal/mol for folding. Because solvent (D_2O) friction could produce an apparent energetic barrier as large as ~ 4.5 kcal/mol,⁴⁷ this result suggests that the intrinsic enthalpic barrier encountered during ^DPDP-II folding is small.

Although the relaxation kinetics of ^DPDP-II can be described by a single-exponential function and is thus consistent with a two-state folding scenario, a downhill folding mechanism cannot be ruled out. Hagen⁴⁸ has shown that an ensemble of conformations diffusing on a one-dimensional downhill free energy surface could result in folding kinetics that are practically indistinguishable from single-exponential or two-state folding kinetics. Therefore, we have also analyzed our *T*-jump results in the context of downhill folding wherein only one conformational ensemble is populated at a given temperature. Muñoz has discussed such downhill folding processes by employing a single-well potential,⁴⁹ where strong deviation from cooperative thermodynamics is expected.^{20,49}

Specifically, we have attempted to quantitatively reproduce the *T*-jump induced relaxation kinetics of ^DPDP-II using Langevin dynamics simulation⁵⁰ in the high friction limit.^{2,21,22} Similar to those used in other studies,^{2,21,22,49} two single-well free energy surfaces corresponding to the initial and final temperatures, respectively, were constructed for a given *T*-jump experiment using eq 2, where *q* represents a putative folding coordinate that could be interpreted as the structural similarity to the native state. Although protein folding occurs on a multidimensional free energy landscape, it has been shown that for minimally frustrated sequences a low-dimensional (one or two) reaction coordinate can quantitatively describe their folding rates.⁵¹ In addition, a recent simulation study also suggests that a single folding conformational coordinate is likely to properly describe β -hairpin folding processes.⁵² To better mimic the experimental conditions, the temperature-dependent native bias

(43) Guo, Z.; Thirumalai, D. *Biopolymers* **1995**, *36*, 83–102.

(44) McCallister, E. L.; Alm, E.; Baker, D. *Nat. Struct. Biol.* **2000**, *7*, 669–673.

(45) Jäger, M.; Nguyen, H.; Crane, J. C.; Kelly, J. W.; Gruebele, M. *J. Mol. Biol.* **2001**, *311*, 373–393.

(46) Krieger, F.; Möglich, A.; Kiefhaber, T. *J. Am. Chem. Soc.* **2005**, *127*, 3346–3352.

(47) Cho, C. H.; Urquidi, J.; Singh, S.; Robinson, G. W. *J. Phys. Chem. B* **1999**, *103*, 1991–1994.

(48) Hagen, S. J. *Proteins* **2003**, *50*, 1–4.

(49) Muñoz, V. *Int. J. Quantum Chem.* **2002**, *90*, 1522–1528.

(50) Veitshans, T.; Klimov, D. K.; Thirumalai, D. *Folding Des.* **1996**, *2*, 1–22.

(41) Roder, H.; Colón, W. *Curr. Opin. Struct. Biol.* **1997**, *7*, 15–28.

(42) Das, C.; Nayak, V.; Raghobhama, S.; Balaram, P. *J. Peptide Res.* **2000**, *56*, 307–317.

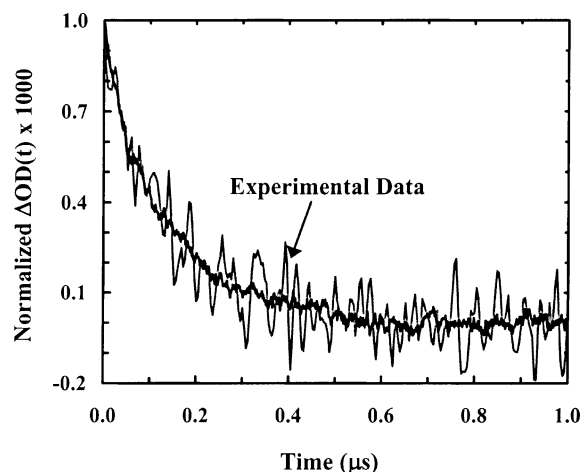


Figure 6. Comparison between the experimental data (gray) and those (black) obtained from a Langevin dynamics simulation for the relaxation kinetics in response to a T -jump from 25.4 to 35.0 °C.

of these free energy surfaces was adjusted using $A(T)$ in such a way that the total β -sheet content of the equilibrium population at each temperature matches that obtained from the FTIR analysis (i.e., those presented in Figure 2). To do so, we have assumed that any conformation with $q > 0.7$ would produce the characteristic amide I' features of antiparallel β -sheet; and the resultant $A(T)$ exhibits a linear temperature dependence in the temperature range of 20 – 60 °C, i.e., $A(T, \text{°C}) = -3.086 + 0.0577T$. Although such an assumption is somewhat arbitrary and has been used in other T -jump studies,^{2,21,22} the choice of the cutoff along q does not affect the results discussed below. In response to a T -jump perturbation, the structural ensemble of interest diffuses toward the new equilibrium position and the dynamics of this population redistribution was evaluated by numerically solving eq 3.

The first type of simulation was carried out using smooth free energy surfaces, which essentially uses the effective diffusion constant (D^*) to account for the roughness of the folding energy landscape or the averaged effect exerted by many degrees of freedom, including those from the solvent, on the conformational diffusion process.^{2,18} As shown (Figure 6), the measured relaxation kinetics (the slow phase) in response to a T -jump of 25.4 to 35.0 °C can be described by a diffusive process with an effective diffusion constant of 0.002 nm²/ns, a value similar to that (0.001 nm²/ns) obtained for a mutant of λ -repressor at 63 °C.² Although friction or energetic roughness can arise from various effects, such as nonnative interactions or native interactions in the wrong topology as well as side chain steric effects, their specific contribution cannot be explicitly determined by the current method. However, simulations carried out at different temperatures may allow us to further estimate the magnitude of the roughness of the one-dimension free energy profile used in this study. As shown (Figure 7a), the resultant effective diffusion constant exhibits a nonlinear temperature dependence and appears to follow the relationship suggested by Zwanzig,⁵³ i.e., $D^* = D_0 \cdot \exp(-(\epsilon/k_B T)^2)$ with an ϵ of about 2.4 kcal/mol (Figure 7b) where both D_0 and ϵ were treated as

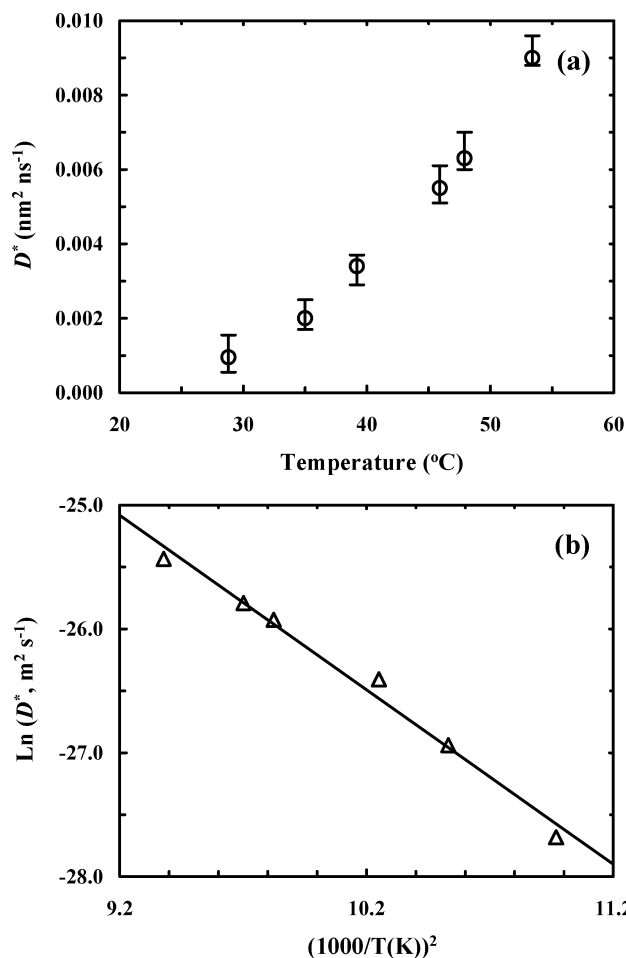


Figure 7. (a) Effective diffusion constant (D^*) vs temperature. (b) Logarithm of D^* vs $(1000/T)^2$.

temperature-independent constants. Considering the fact that the temperature dependence of the solvent (D_2O) viscosity could produce an apparent activation energy of about 4.5 kcal/mol,⁴⁷ these results suggest that interactions with the solvent molecules are important determinants of the roughness of the folding free energy landscape of ^{DPDP}–II, which play a more pronounced role in retarding the conformational motion at low temperatures. Consistent with our observations, García and Sanbonmatsu⁵⁴ as well as Zhou and co-workers^{55,56} have shown that the roughness of the folding energy landscape of β -hairpin GB1^{54,55} and miniprotein Trp-cage⁵⁶ decreases with increasing temperature. Similarly, Wolynes and co-workers have shown that specific water-mediated interactions can affect the folding funnel of a protein in a significant way.⁵⁷

In the second type of simulation, we sought to use random Gaussian noise to mimic the residual roughness (i.e., ΔG_{ran} in eq 2) of the folding free energy surface, which fluctuates with time. Because the root-mean-square of the free energy fluctuation, δG , and the diffusion constant (D) are interrelated, they cannot be independently determined using the current approach. Therefore, we assumed that the conformational diffusion

(51) Nymeyer, H.; Socci, N. D.; Onuchic, J. N. *Proc. Natl. Acad. Sci. U.S.A.* **2000**, *97*, 634–639.

(52) Daidone, I.; D'Abramo, M.; Di, Nola, A.; Amadei, A. *J. Am. Chem. Soc.* **2005**, *127*, 14825–14832.

(53) Zwanzig, R. *Proc. Natl. Acad. Sci. U.S.A.* **1988**, *85*, 2029–2030.

(54) García, A. E.; Sanbonmatsu, K. Y. *Proteins Struct. Funct. Genet.* **2001**, *42*, 345–354.

(55) Zhou, R.; Berne, B. J.; Germain, R. *Proc. Natl. Acad. Sci. U.S.A.* **2001**, *98*, 14931–14936.

(56) Zhou, R. *Proc. Natl. Acad. Sci. U.S.A.* **2003**, *100*, 13280–13285.

(57) Papoian, G. A.; Ulander, J.; Eastwood, M. P.; Luthey-Schulten, Z.; Wolynes, P. G. *Proc. Natl. Acad. Sci. U.S.A.* **2004**, *101*, 23352–23357.

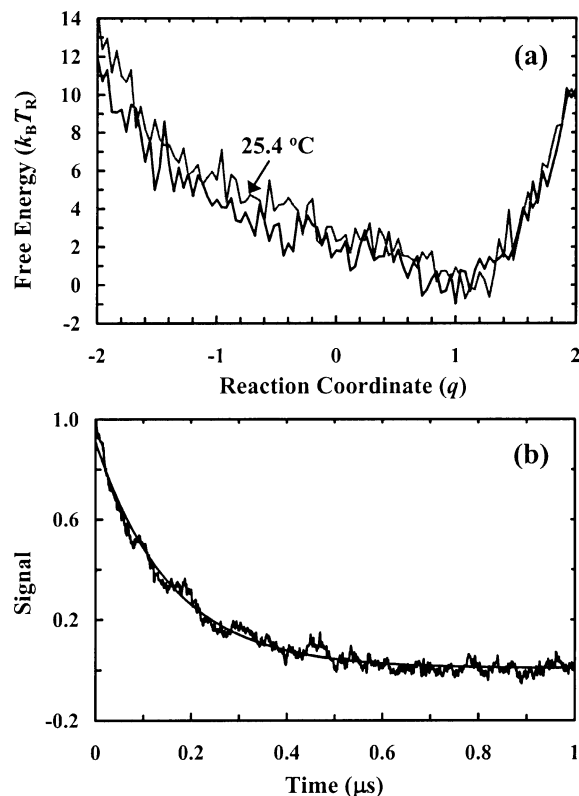


Figure 8. (a) Free energy profiles used in the Langevin dynamics simulation for 25.4 °C (gray) and 35.0 °C (black), respectively. For both surfaces, $\delta G \approx 0.7 k_B T$. (b) Simulated T -jump induced relaxation data at 35.0 °C. The smooth line is a single-exponential fit to these data.

constant of $^{\text{D}}\text{P}^{\text{D}}\text{P-II}$ is similar to that measured for relative motions between two positions along a polypeptide chain of similar length,^{30,31} and have used a value of $0.04 \text{ nm}^2/\text{ns}$ for D in the calculation. A similar value has also been used by Yang and Gruebele in describing the downhill folding behaviors of a five-helix bundle protein.²¹ As shown (Figure 8), the resultant δG from Langevin dynamics simulations that yielded relaxation kinetics matching those measured from experiments is $\sim 0.7 k_B T$ at 35.0 °C and $\sim 0.5 k_B T$ at 45.9 °C, respectively. Interestingly, the estimated δG for $^{\text{D}}\text{P}^{\text{D}}\text{P-II}$ is smaller than that ($0.8 k_B T$) measured for λD14A at 63 °C,²¹ indicative of the important effect of the polypeptide chain length. In addition, this result may also be compared with that ($1.7 k_B T$) inferred from the rate of loop closure in model peptides by Lapidus and co-workers.⁵⁸

It has been suggested that a downhill folding process would lead to stretched exponential kinetics, especially when the roughness of the folding energy landscape increases as folding proceeds.^{59,60} However, the diffusion dynamics of $^{\text{D}}\text{P}^{\text{D}}\text{P-II}$ can be adequately described by a single-exponential function (Figure 8b). This is consistent with the study of Hagen⁴⁸ and indicates

that the observation of first-order folding kinetics is not sufficient to exclusively determine the mechanism of folding, although a two-state scenario always results in single-exponential folding as well as relaxation kinetics. In addition, this result is in agreement with the studies of Zwanzig⁵³ and Yang and Gruebele.²¹ They have suggested that conformational diffusions along a folding coordinate with uncorrelated roughness and a strong bias toward the native state can be described by single-exponential kinetics because the barrier is completely dominated by the residual roughness along the free energy surface.²¹ Therefore, the single-exponential relaxation behaviors observed for $^{\text{D}}\text{P}^{\text{D}}\text{P-II}$ and the random free energy fluctuations used in the Langevin dynamics simulations are self-consistent.

It is worth pointing out that even though the current study does not allow us to pinpoint the magnitude of the folding free energy barrier, it nevertheless allows us to set limits on several important physical parameters regarding the folding process of β -sheets. For example, it clearly demonstrated that the “attempting” frequency for folding of β -sheets with similar size should be on the order of $(0.1\text{--}0.3 \mu\text{s})^{-1}$, a value well within the range estimated by Li et al.⁶¹

Conclusion

In summary, we have studied the folding thermodynamics and kinetics of a 20-residue peptide, $^{\text{D}}\text{P}^{\text{D}}\text{P-II}$. It folds into a three-stranded antiparallel β -sheet and possesses rather unique folding properties because its turn sequences contain a $^{\text{D}}\text{PG}$ segment. The latter is known to facilitate the formation of stable β -turns that are resistant to highly denatured conditions. The folding of this peptide is expected to occur on a very fast time scale because it has been shown that the turn formation plays an important role in controlling the folding free energy barrier of β -hairpins. Indeed, the T -jump induced relaxation kinetics, probed by infrared spectroscopy, proceed on the nanosecond time scale, indicating that the T -jump induced conformational relaxation encounters either a relatively small, two-state folding free energy barrier or no distinct barriers at all. Without making further effort to distinguish these two possibilities, we employed two theoretical models to analyze those T -jump kinetic data. A simple two-state analysis yielded both folding and unfolding rate constants for this β -sheet. As it is expected, $^{\text{D}}\text{P}^{\text{D}}\text{P-II}$ folds with an exceedingly fast rate, e.g., $(0.26 \pm 0.02 \mu\text{s})^{-1}$ at room temperature. In the second analysis, we assumed that the conformational relaxation dynamics of $^{\text{D}}\text{P}^{\text{D}}\text{P-II}$ could be described by diffusion motions on a single-well free energy surface. Consequently, Langevin dynamics simulations allowed us to estimate the effective diffusion constant of the diffusion motion corresponding to specific experimental conditions. Interestingly, our results suggest that residual roughness of the free energy surface arises mainly from interactions between the peptide and solvent molecules.

Acknowledgment. We thank the NIH (GM065978) for funding.

JA064865+

(58) Lapidus, L. J.; Eaton, W. A.; Hofrichter, J. *Proc. Natl. Acad. Sci. U.S.A.* **2000**, *97*, 7220–7225.

(59) Hagen, S. J.; Eaton, W. A. *J. Chem. Phys.* **1996**, *104*, 3395–3398.

(60) Socci, N. D.; Onuchic, J. N.; Wolynes, P. G. *J. Chem. Phys.* **1996**, *104*, 5860–5868.

(61) Li, M. S.; Klimov, D. K.; Thirumalai, D. *Polymer* **2004**, *45*, 573–579.